J Physiol 586.20 (2008) pp 4859–4875

The Journal of Physiology

Depletion of calcium stores regulates calcium influx and signal transmission in rod photoreceptors

Tamas Szikra[1], Karen Cusato[1], Wallace B. Thoreson[2,3], Peter Barabas[4], Theodore M. Bartoletti[3] and David Krizaj[1,4,5]

[1]*Department of Ophthalmology, UCSF School of Medicine, San Francisco, CA 94143, USA*
[2]*Department of Ophthalmology & Visual Sciences, University of Nebraska Medical Center, Omaha, NE 68198, USA*
[3]*Department of Pharmacology and Experimental Neurosciences, University of Nebraska Medical Center, Omaha, NE 68198, USA*
[4]*Department of Ophthalmology & Visual Sciences and* [5]*Department of Physiology, University of Utah School of Medicine, Salt Lake City, UT 84132, USA*

Tonic synapses are specialized for sustained calcium entry and transmitter release, allowing them to operate in a graded fashion over a wide dynamic range. We identified a novel plasma membrane calcium entry mechanism that extends the range of rod photoreceptor signalling into light-adapted conditions. The mechanism, which shares molecular and physiological characteristics with store-operated calcium entry (SOCE), is required to maintain baseline $[Ca^{2+}]_i$ in rod inner segments and synaptic terminals. Sustained Ca^{2+} entry into rod cytosol is augmented by store depletion, blocked by La^{3+} and Gd^{3+} and suppressed by organic antagonists MRS-1845 and SKF-96365. Store depletion and the subsequent Ca^{2+} influx directly stimulated exocytosis in terminals of light-adapted rods loaded with the activity-dependent dye FM1–43. Moreover, SOCE blockers suppressed rod-mediated synaptic inputs to horizontal cells without affecting presynaptic voltage-operated Ca^{2+} entry. Silencing of TRPC1 expression with small interference RNA disrupted SOCE in rods, but had no effect on cone Ca^{2+} signalling. Rods were immunopositive for TRPC1 whereas cone inner segments immunostained with TRPC6 channel antibodies. Thus, SOCE modulates Ca^{2+} homeostasis and light-evoked neurotransmission at the rod photoreceptor synapse mediated by TRPC1.

(Received 18 July 2008; accepted after revision 27 August 2008; first published online 28 August 2008)
Corresponding author D. Krizaj: Department of Ophthalmology & Visual Sciences, Moran Eye Center, University of Utah School of Medicine, Salt Lake City, UT 84132, USA. Email: david.krizaj@hsc.utah.edu

Tonic neurotransmission at vertebrate rod synapses is sustained by continuous dark Ca^{2+} influx into rod terminals (reviewed in Heidelberger *et al.* 2005). Light-evoked hyperpolarization closes L-type voltage-operated channels in the rod terminal causing a decrease in presynaptic $[Ca^{2+}]_i$ and suppression of exocytosis (Choi *et al.* 2005). The amplitude and kinetics of $[Ca^{2+}]_i$ and neurotransmission at rod synapses are additionally modulated by PMCA-mediated extrusion (Duncan *et al.* 2006; Yang *et al.* 2007) and by ryanodine receptor-mediated Ca^{2+} release from internal stores (Suryanarayanan & Slaughter, 2006; Cadetti *et al.* 2006). However, whereas depolarization-evoked glutamate release from rods is completely suppressed by L-type channel antagonists that block voltage-dependent Ca^{2+} entry (Schmitz & Witkovsky, 1997), saturating white light blocks only a fraction of total released glutamate (Schmitz & Witkovsky, 1996). This suggests that the dynamic range of rod signalling is regulated by another, voltage-independent Ca^{2+} influx pathway that is activated in light-adapted, strongly hyperpolarized cells.

In many types of cell, Ca^{2+} loss from ER stores triggers subsequent Ca^{2+} influx through plasma membrane store-operated channels (SOC channels) (reviewed in Parekh & Putney, 2005). The influx is activated by targeted migration of EF-hand proteins STIM1 and STIM2 to ER cisternae puncta located underneath the membrane (Roos *et al.* 2005; Brandman *et al.* 2007). The stoichiometry of these complexes may vary across different types of cell, but has been proposed to include various combinations of Orai1 and TRPC protein families (Liao *et al.* 2007; Worley *et al.* 2007; Chen *et al.* 2008). Although SOCE has been identified in some excitable cells (Garaschuk *et al.* 1997; Usachev & Thayer, 1999) that include embryonic retinal neurons (Sakaki *et al.* 1997) and retinal amacrine

This paper has online supplemental material.

DOI: 10.1113/jphysiol.2008.160051

cells (Borges *et al.* 2008), the identity and functional significance of neuronal SOC channels is still intensely debated.

Two families of Ca^{2+}-permeable ion channels have been implicated in SOCE. The Orai channel family has been shown to mediate SOCE through the well-known lymphocyte CRAC channel (Feske *et al.* 2006; Vig *et al.* 2008). In addition, studies in heterologously expressing systems and in animal knockout models have strongly implicated the TRPC1 isoform homologous to TRP (transient receptor potential) proteins originally cloned from *Drosophila* photoreceptors in SOCE. The present report aims to characterize a novel Ca^{2+} entry pathway in vertebrate rod photoreceptors that is facilitated by depletion of intracellular Ca^{2+} stores. We show that this pathway regulates baseline $[Ca^{2+}]_i$ in hyperpolarized rods and suggest that SOCE in rods is mediated in part by the TRPC1 channel, whereas cones express a different TRPC isoform. Taken together, our study suggests that intracellular stores play an important role in information processing in vertebrate vision, both directly through Ca^{2+} release and sequestration and indirectly through modulation of plasma membrane Ca^{2+} entry. In addition, we have identified another, potentially significant, difference in Ca^{2+} signalling between rods and cones.

Methods

$[Ca^{2+}]_i$ concentration was measured in cells loaded with the fluorescent indicator fura-2 as reported previously (Szikra & Krizaj, 2006). Neotenic tiger salamanders (*Ambystoma tigrinum*) were decapitated and pithed using procedures approved by the UCSF and University of Utah Committees for Animal Care and in accordance with the National Institute of Health Guide for the Care and Use of Laboratory Animals. Retinas were dissected from enucleated eyes, and dissociated in 0 Ca^{2+}/papain (10 U ml^{-1}; Worthington, Freehold, NJ, USA) saline for 20 min at room temperature (20–22°C). The retina was cut into small pieces and dissociated prior to the experiment. Cells were plated onto coverslips coated with 0.2 mg ml^{-1} concanavalin A (Sigma, St Louis, MO, USA). The recording chamber was superfused via two electronically controlled multi-inlet manifolds (MP-6 and MP-8, Warner Instruments, Hamden, CT, USA). The control saline solution contained (in mM): 97 NaCl, 2 KCl, 2 $CaCl_2$, 2 $MgCl_2$, 10 Hepes, 2 lactic acid, 0.3 ascorbic acid and 1 taurine at 240 mosmol l^{-1}. pH was adjusted to 7.6 with NaOH. To stimulate glycolysis, the glucose concentration in the saline was 20 mM. All chemicals were obtained from Sigma. TRPC1 RNAi was custom designed by Cenix Bioscience/ Ambion (Austin, TX, USA) with the following sequence: sense: CCACUUUGGAUGAAAGGCUtt; antisense: AGCCUUUCAUCCAAAGUGGtc, based on the TRPC1 sequence from *Xenopus laevis* (UniGene accession number XI.470). Silencer® negative control RNAi, proven to have minimal effects on cell viability, was purchased from Ambion.

To prepare retinal slices for electrophysiological experiments, a section of eyecup was placed vitreal side down on a piece of filter paper (2 × 5 mm, Type AAWP, 0.8 μm pores, Millipore, Bedford, MA, USA) and isolated in cold saline solution. Slices were prepared under infrared illumination using Gen-III image intensifiers (Nitemate NAVe, Litton Industries, Tempe, AZ, USA). Retinal slices (125 μm) were cut with a razor blade tissue chopper (Stoelting, Wood Dale, IL, USA) and placed in a recording chamber for viewing of the retinal layers with an upright fixed stage microscope (Olympus BHWI, Tokyo, Japan with 40×, 0.7 NA objective or Nikon E600 FN, Japan with 60×, 1.0 NA objective). Slices were superfused at ~1 ml min^{-1} with an oxygenated solution containing (in mM): 111 NaCl, 2.5 KCl, 1.8 $CaCl_2$, 0.5 $MgCl_2$, 10 Hepes, 5 glucose, 0.1 picrotoxin, 0.001 strychnine (pH 7.8).

$[Ca^{2+}]_i$ measurements. Isolated photoreceptors were loaded with 2–5 μM fura-2 AM (fura 2-acetoxymethylester; Molecular Probes, Eugene, OR, USA) for 10 min and subsequently washed for 20 min. This indicator has a dissociation constant (K_d) of 224 nM (Neher, 1995) which is close to resting $[Ca^{2+}]_i$ and provides large changes in signal for $[Ca^{2+}]_i$ starting from resting levels in light-adapted cells (Krizaj & Copenhagen, 1998). Fluorescence signals were acquired on an inverted microscope (Nikon Eclipse 200) using a dry 40× objective (NA = 0.8) or an oil 100× objective (NA = 1.2). The regions of interest (ROI) were positioned onto the cell body of rods and cones (here termed 'IS'), unless otherwise indicated. In a subset of experiments, data were acquired simultaneously from the synaptic terminal, cell body and ellipsoid regions of the IS. Image acquisition was generally binned at 3 × 3 pixels (except for Fig. 2 where the binning was 2 × 2) and was run at 0.5–1 Hz by a cooled 12 bit digital CCD camera (Cascade 650, Photometrics, Tucson, AZ, USA). The camera and the shutter were controlled by commercial software (Metafluor 6.1; Universal Imaging, West Chester, PA, USA). $[Ca^{2+}]_i$ was calculated by measuring the ratio of the two emission intensities for excitation at 340 and 380 nm after subtraction of the background fluorescence and imported into a data analysis program (Igor Pro, Wavemetrics, Lake Oswego, OR, USA) used to calculate the concentration of free $[Ca^{2+}]_i$ in the cytosol. The decay time constant was calculated by fitting single exponentials to the decrease of $[Ca^{2+}]_i$ in the presence of 0 $[Ca^{2+}]_o$ with Igor Pro (Szikra & Krizaj, 2007).

Free $[Ca^{2+}]$ levels were calibrated *in vivo* with 10 μM ionomycin in 0 and 10 mM $[Ca^{2+}]_o$ saline using the standard relationship (Grynkiewicz *et al.* 1985). We were occasionally unable to calibrate $[Ca^{2+}]_i$ levels; therefore, data for some cells are presented as 340/380 nm ratios. It is possible that the intracellular environment caused small changes in Ca^{2+} binding to fura-2, which would be expected to change the K_d parameter (Grynkiewicz *et al.* 1985). All pooled data are presented as means ± S.E.M. Significance was determined using Student's *t* test.

FM1–43 staining. The experimental protocol was adopted from Rea *et al.* (2004). Briefly, neotenic tiger salamanders were dark-adapted before enucleation. Eyes were dissected under infrared light using IR goggles attached to a dissecting microscope. Whole retinas were placed in normal Ringer solution containing 2 mM $[Ca^{2+}]_o$ and loaded with FM1–43 dye (30 μM) in the dark for 30 min. Excess dye was removed by washing the retinas with 1 mM Advasep-7 for 10 min. Loaded retinas were treated with 0 Ca^{2+}/papain solution as described above. Small pieces of retinas were kept in 0 Ca^{2+} solution. Retina pieces were dissociated by gentle pipetting. Ca^{2+} was re-introduced during the experiment and the fluorescence drop was monitored. Maximal release of vesicles was achieved by the application of 30 mM KCl. Upon depolarization the maximum signal was normalized to 1.0 at the onset of the experiment. Minimum signal was normalized to 0 at the end of experiment. The amplitude of SOCE-evoked fluorescence drop was normalized to the KCl-evoked signal.

Electrophysiology. Whole-cell recordings were obtained using 8–15 MΩ patch electrodes pulled from borosilicate glass (1.2 mm o.d., 0.95 mm i.d., with internal filament, World Precision Instruments, Sarasota, FL, USA) on a PP-830 micropipette puller (Narishige USA, East Meadow, NY, USA). The pipette solution contained (in mM): 94 caesium gluconate, 9.4 TEA-Cl, 1.9 $MgCl_2$, 9.4 MgATP, 0.5 GTP, 5 EGTA, 32.9 Hepes (pH 7.2). The osmolarity was measured with a vapor pressure osmometer (Wescor, Logan, UT, USA) and adjusted, if necessary, to ∼242 mosmol l^{-1}.

Rods were voltage clamped at −70 mV and horizontal cells at −60 mV using a Multiclamp patch-clamp amplifier (Axon Instruments, Union City, CA, USA). Recording pipettes were positioned with Huxley–Wall micromanipulators (Sutter Instruments, Novato, CA, USA). Currents were acquired using a Digidata 1322 interface and pCLAMP 9.2 software (Axon Instruments). Cell types were distinguished by morphological and physiological criteria (Thoreson *et al.* 1997). Passive cell properties were similar to those reported by Cadetti *et al.* (2005). Charging curves for rods and many horizontal cells could be fitted by single exponentials, indicating a compact electrotonic structure and suggesting that horizontal cells were largely uncoupled from their neighbours in the retinal slice preparations used for these studies.

Light stimuli were generated by a tungsten light source; intensity was controlled by Wratten gel neutral density filters and wavelength by interference filters. Rod-dominated light responses were evoked by using 580 nm light flashes applied to dark-adapted retina. Spectral measurements indicate that horizontal cells in the amphibian retinal slice preparation receive predominantly rod inputs under these conditions (Thoreson *et al.* 2003). Strong rod input was further indicated by the slow recovery of dark-adapted responses, mirroring the slow recovery of rod responses, at offset of the 580 nm stimulus.

Immunostaining. Immunostaining procedures were performed as described (Krizaj *et al.* 2003). Fixed transverse sections of the retina were washed in phosphate buffer (PB) for 15 min before permeabilization and blocked in 0.5% Triton X-100 and 10% goat serum. Below we provide details of antibody production and tests of antibody specificity. Polyclonal antibodies against two members of the canonical transient receptor potential family (TRPC1 and 6) were raised in rabbit against synthetic peptides (Chemicon-Millipore, Temecula, CA, USA), as follows: amino acids 557–571 from human TRPC1 (accession P48995); amino acids 24–38 from mouse TRPC6 (accession Q61143). A rabbit polyclonal TRPC1 antibody was purchased from Sigma (T8276; raised against amino acids 557–571 of human TRPC1; accession P48995). A mouse polyclonal antibody raised against human TRPC1 was a generous gift from Dr Leonidas Tsiokas (University of Oklahoma Health Science Center; Ma *et al.* 2003). The secondary antibodies utilized were goat anti-mouse or goat anti-rabbit IgG (H + l) conjugated to fluorophores (Alexa 488 and Alexa 594 conjugates (Invitrogen), diluted 1 : 500 or 1 : 1000 or goat anti-mouse Cy3 from Jackson ImmunoResearch Laboratories (West Grove, PA, USA) at 1 : 1000. After incubation, sections on slides were washed in PB and mounted with Vectashield (Vector Laboratories, Burlingame, CA, USA). Negative controls for non-specific staining of secondary antibodies were performed for every set of experiments by omitting the primary antibodies and specific neutralizing antibodies were co-incubated with primary antibodies to test for specificity of binding. Immunofluorescence and differential interference contrast (DIC) images were acquired at depths of 12 bits on a confocal microscope (Zeiss LSM5 Pascal or Zeiss LSM 510) using 488 nm Ar and 594 nm He/Ne lines for fluorophore excitation, suitable band-pass or long-pass filters for emission detection, and a 40×/1.2 NA oil or 63×/0.9 NA water objectives.

RNAi incubation. Salamander eyes were removed following decapitation, and were rinsed 2× in sterile filtered L-15. Retinas were isolated and four small radial cuts were made. Retinas were flat-mounted, photoreceptors facing up on Millicell-cm (Millipore) culture inserts in 35 mm culture dishes that contained 1 ml of L-15.

Retinas were transfected with RNAi using Transfectin reagent (Bio-Rad Laboratories, Hercules, CA, USA) according to the manufacturer's instructions. Briefly, 2 μl of Transfectin was diluted in 100 μl of L-15, and 1.2 μl of fluorescein-conjugated RNAi for TRPC1 (from stock of 200 mM; Ambion) was diluted in 100 μl of L-15. Transfectin and RNAi were combined and incubated at room temperature for 20 min. The RNAi solution was placed directly on top of the culture insert with an additional 200 μl of L-15 from the dish. The final volume of medium was 1.2 ml and the final concentration of RNAi was 200 nM. Retinas were cultured for 24 or 48 h at 13°C. Retinas were enzymatically dissociated for calcium imaging as described above or flash frozen for protein extraction and Western blotting.

Some retinas were fixed for immunostaining in 4% paraformaldehyde. Others were imaged by confocal microscopy or cells were isolated for calcium imaging.

Statistics. All pooled data are presented as means ± S.E.M. The significance of results from experiments involving populations of cells was evaluated with Student's *t* test for unpaired data. Pre- and post-drug treatment pairs for those samples were tested by a *t* test for paired data. The significance of means of three different treatments was determined with one-way ANOVA and Bonferrioni's *post hoc* and Dunnett's test. The degree of significance is indicated by asterisks: $^{*}P < 0.05$; $^{**}P < 0.001$; $^{***}P < 0.0001$.

Results

Intracellular Ca^{2+} concentration in light-adapted salamander rod photoreceptors was monitored in cells loaded with the high affinity Ca^{2+} indicator fura-2. This non-invasive approach ensured that important cytosolic molecules potentially involved in modulation of Ca^{2+} fluxes were not lost or compromised. Subsequently, the signalling mechanisms identified in isolated cells were tested in retinal slices using simultaneous recordings from rods and postsynaptic neurons.

Light-adapted rods experience sustained Ca^{2+} entry from the extracellular space

Bright light closes voltage-operated Ca^{2+} channels in regions downstream from the rod outer segment (the 'inner segment'), resulting in $[Ca^{2+}]_{IS}$ decrease from several hundred nanomolar observed in depolarized rods to several tens of nanomolar measured in light-adapted cells (Krizaj & Copenhagen, 1998; Choi *et al.* 2005). Baseline $[Ca^{2+}]_i$ declined further still when light-adapted cells were exposed to low or Ca^{2+}-free saline. $[Ca^{2+}]_i$ decreased from 51 ± 3 nM in control light-adapted cells, to 16 ± 2 nM in Ca^{2+} free saline ($n = 45$, $P < 0.0001$) (Fig. 1*A*, see also Figs 2*A–C* and 3*C*) with a time constant of decay of 81 ± 13 s ($n = 13$). The decrease in $[Ca^{2+}]_i$ under conditions when voltage-operated Ca^{2+} channels in the IS are closed suggests a novel sustained mechanism of plasma membrane Ca^{2+} entry operates in light-adapted hyperpolarized rods.

Consistent with this hypothesis, when the driving force for Ca^{2+} influx in hyperpolarized rods was modulated by changing the extracellular calcium concentration $[Ca^{2+}]_o$, the direction of baseline $[Ca^{2+}]_i$ followed changes in $[Ca^{2+}]_o$. An increase in $[Ca^{2+}]_o$ from 2 to 10 mM elevated cytosolic $[Ca^{2+}]_i$ to 133 ± 19 nM, whereas a decrease to 1 mM lowered $[Ca^{2+}]_i$ by 36% to 27 ± 5 nM ($n = 8$, $P < 0.05$; Figs 1*B* and Fig. 2*E*, dotted trace). Baseline $[Ca^{2+}]_i$ recovered to control levels following re-perfusion with control 2 mM Ca^{2+}-containing saline.

To determine the mechanism of Ca^{2+} entry into hyperpolarized rods, ISs were bathed with wide-spectrum Ca^{2+} channel antagonists La^{3+} and Gd^{3+}. At micromolar concentrations, the two lanthanides block several classes of Ca^{2+}-permeable voltage-gated plasma membrane channels yet have little effect on Ca^{2+} transporters such as PMCA that provide the exclusive Ca^{2+} extrusion pathway in the rod IS (Krizaj & Copenhagen, 2002). As shown in Fig. 1*C*, La^{3+} (10 μM) and Gd^{3+} (10 μM) reduced $[Ca^{2+}]_i$ baseline to levels comparable to those observed in Ca^{2+} free saline (La^{3+}: 16 ± 4 nM; $n = 5$, $P < 0.05$) (Gd^{3+}: 21 ± 3 nM; $n = 6$, $P < 0.05$). These data suggest that the continuous Ca^{2+} influx into light-adapted rods observed might occur through Ca^{2+}-permeable channels.

The main pathway for Ca^{2+} entry into salamander rod IS cytosol is L-type Ca^{2+} channels (Bader *et al.* 1982), whereas cone ISs also express CNG channels (Rieke & Schwartz, 1994). However, application of the CNG antagonist L-*cis*-diltiazem (100 μM), the L-type Ca^{2+} channel agonist FPL 64176 (10 μM) and L-type channel antagonist nifedipine (2 μM) produced no significant changes in $[Ca^{2+}]_i$ baseline (Fig. 1*C*; $n = 7$). Likewise, voltage-gated Ca^{2+} channel antagonist Cd^{2+} had no effect on rod IS baseline at 100 μM (Fig. 1*C*; control 64 ± 9 nM; Cd^{2+} 68 ± 10 nM; $P = 0.8212$; $n = 8$). Consistent with the well-known role for voltage-operated Ca^{2+} entry in depolarized rods, 2 μM nifedipine reduced the amplitude of depolarization-evoked $[Ca^{2+}]_i$ increases by 70–100% (Szikra & Krizaj, 2006) whereas FPL 64176 potentiated the amplitude of depolarization-evoked responses by $474 \pm 96\%$ (Fig. 1*D*, $P < 0.05$). Although

depolarization-evoked influx involves L-type Ca^{2+} channels, these results suggest the continuous Ca^{2+} influx in light-adapted rods is independent of voltage-operated and CNG-dependent Ca^{2+} entry.

The sensitivity of hyperpolarized rod baseline $[Ca^{2+}]_i$ to the Ca^{2+} driving force, trivalent cations and its lack of responsiveness to L-type channel effectors suggest that Ca^{2+} entry into light-adapted cells occurs through a

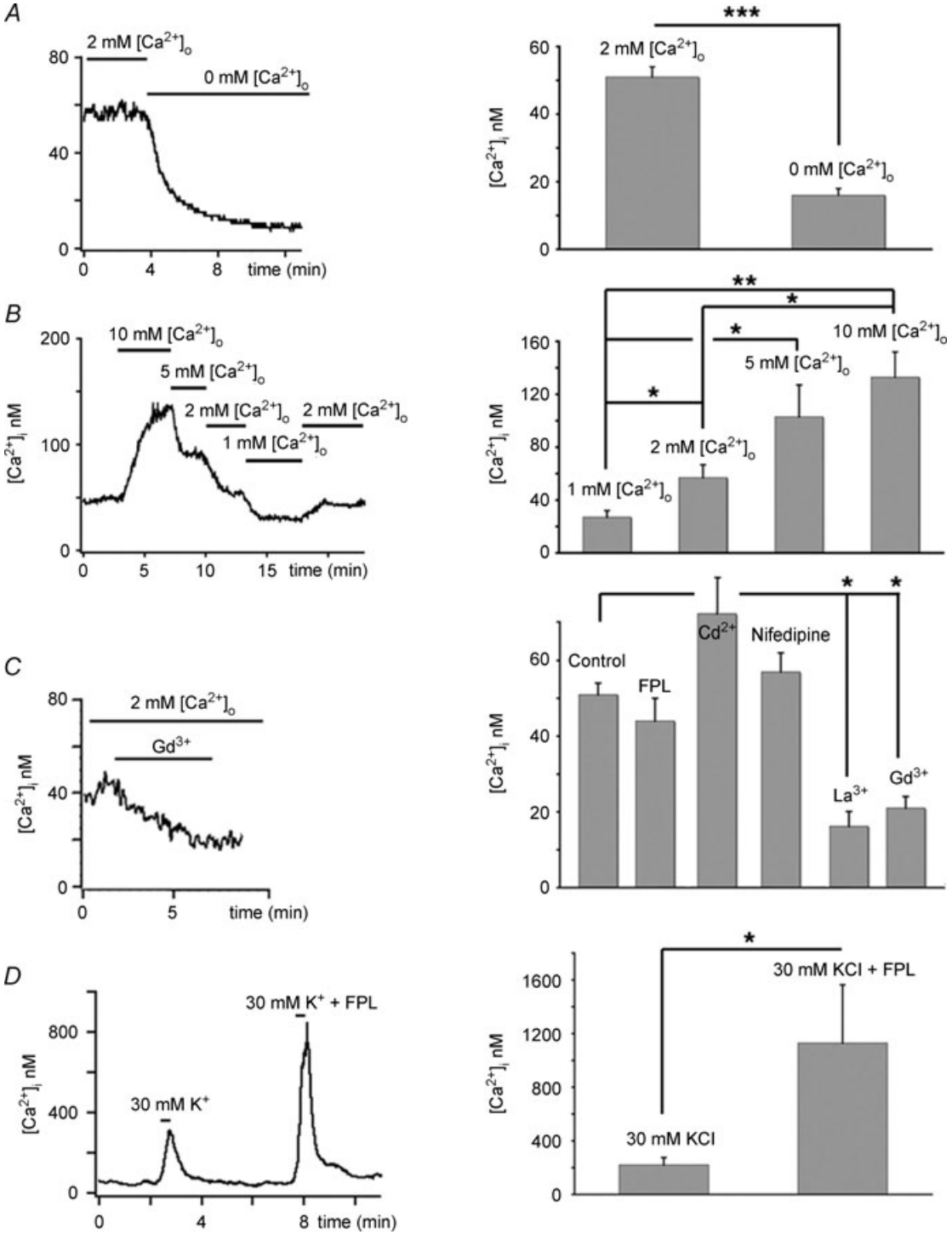

Figure 1. $[Ca^{2+}]_i$ baseline in light adapted rods is sustained by tonic Ca^{2+} influx
A, Ca^{2+} removal from the saline solution results in decrease in $[Ca^{2+}]_i$. *B*, $[Ca^{2+}]_i$ follows changes in the driving force for Ca^{2+} entry as $[Ca^{2+}]_o$ is increased from 1 to 10 mM (*C*). 1 μM Gd^{3+} or La^{3+} decrease baseline $[Ca^{2+}]_i$, whereas agonist (FPL 64176) and antagonists (nifedipine and Cd^{2+}) of L-type voltage-operated Ca^{2+} channels have no significant effect on $[Ca^{2+}]_i$ baseline. *D*, FPL 64176 augmented $[Ca^{2+}]_i$ elevation evoked by 30 mM KCl.

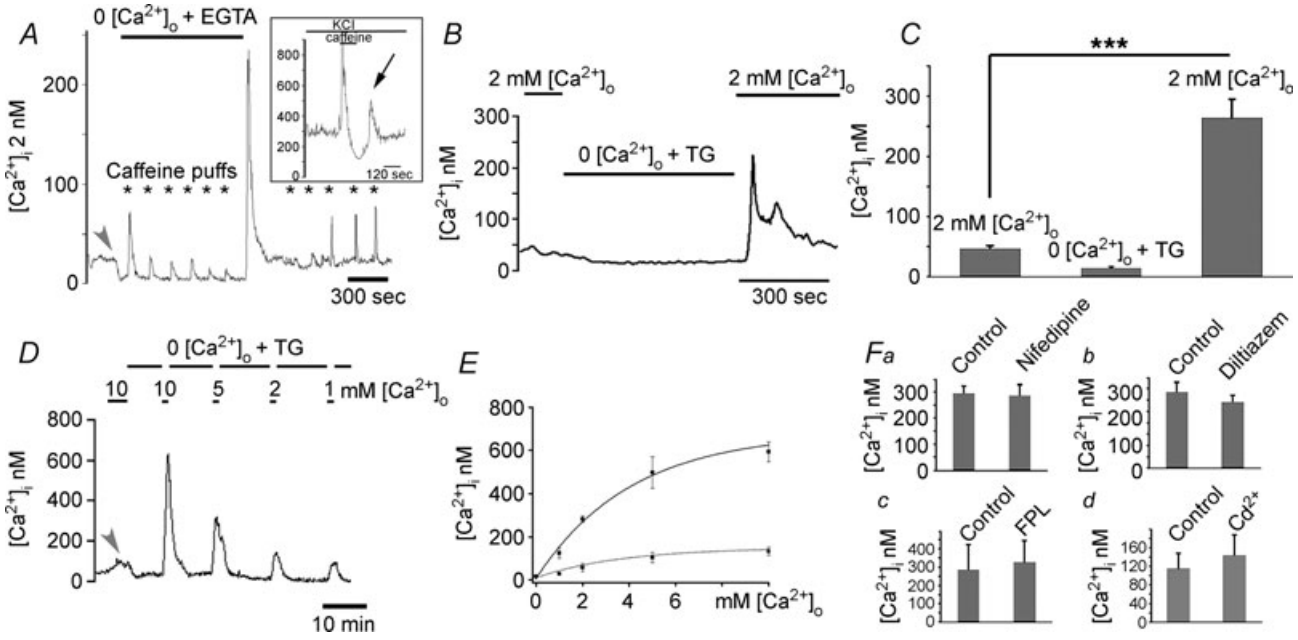

Figure 2. Depletion of Ca^{2+} stores facilitates plasma membrane Ca^{2+} entry
A, deprivation of Ca^{2+} in the saline causes a decrease in baseline $[Ca^{2+}]_i$ (arrow). ER stores were depleted by sequential puffs of 50 mM caffeine (asterisks). Following exposure to control, 2 mM Ca^{2+}-containing saline, $[Ca^{2+}]_i$ exhibited a marked overshoot, which decreased as the stores refilled with Ca^{2+}. Inset: rod depolarized with 20 mM KCl. Depletion of Ca^{2+} stores with 2 min perfusion with 10 mM caffeine caused a large transient increase in $[Ca^{2+}]_i$ due to Ca^{2+} release from ryanodine stores. Following re-addition of control 20 mM KCl-saline, a transient $[Ca^{2+}]_i$ overshoot occurred. *B*, the store depletion protocol. Ca^{2+} stores were depleted in 0 Ca^{2+} saline supplemented with 1 μM thapsigargin. Re-addition of control saline triggered a $[Ca^{2+}]_i$ overshoot. *C*, summary of the data obtained by the depletion protocol. *D*, store depletion potentiates $[Ca^{2+}]_o$-evoked Ca^{2+} entry. Rod, first stimulated with 10 mM $[Ca^{2+}]_o$, was superfused with 0 Ca^{2+}/TG saline. The cell was re-exposed to 10 mM $[Ca^{2+}]_i$, followed by a sequence of overshoots elicited by saline containing 5, 2 and 1 mM $[Ca^{2+}]_o$, respectively. *E*, graphed data for all experiments following sequence shown in *D*. Lower trace represents cells with intact stores upper trace represents cells with depleted stores. *F*, depletion-evoked Ca^{2+} entry does not occur through L-type or CNG Ca^{2+}-permeable channels. Nifedipine (2 μM) (*a*), L-*cis*-diltiazem (100 μM) (*b*), FPL-64176 (10 μM) (*c*) and Cd^{2+} (100 μM) (*d*) had little effect on $[Ca^{2+}]_i$ overshoots.

novel type of plasma membrane Ca^{2+}-permeable channel not previously identified in photoreceptors. Given that in some neurons plasma membrane Ca^{2+} entry occurs through mechanisms that refill Ca^{2+} stores (Usachev & Thayer, 1999) and that ryanodine-sensitive stores significantly contribute to rod IS Ca^{2+} homeostasis (Krizaj *et al.* 1999; Cadetti *et al.* 2006), we investigated plasma membrane Ca^{2+} entry in rods by

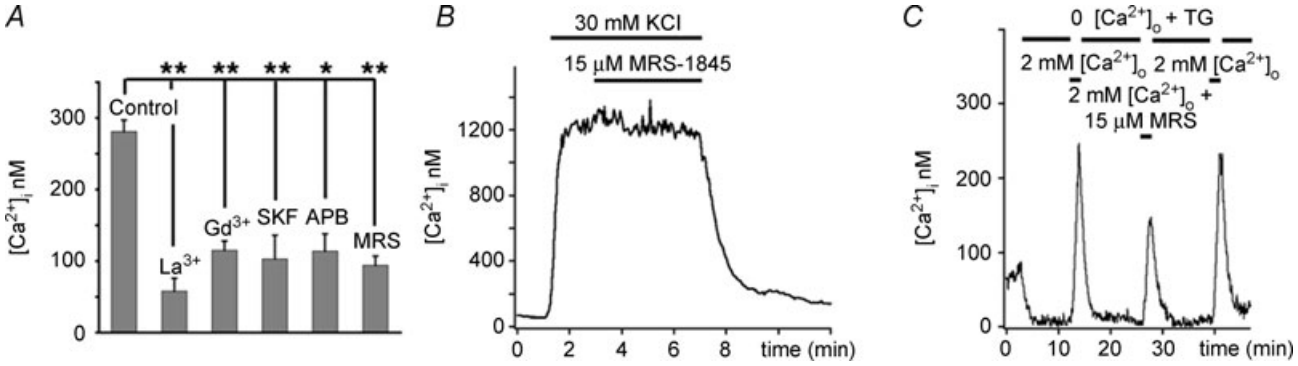

Figure 3. Depletion-evoked Ca^{2+} overshoots are blocked by trivalent cations and organic antagonists of SOCE
A, tabulated data. *B*, rod depolarized with 30 mM KCl. MRS-1845 had no effect on $[Ca^{2+}]_i$ induced by voltage-operated Ca^{2+} entry. *C*, MRS-1845 (15 μM) reversibly suppresses SOCE.

manipulating the Ca^{2+} content of endoplasmic reticulum (ER).

Store-operated Ca^{2+} entry in light-adapted rods

Long-term depletion of ER stores with the irreversible sarcoplasmic-endoplasmic reticulum Ca^{2+}-ATPase (SERCA) inhibitor thapsigargin caused a sustained elevation of baseline $[Ca^{2+}]_i$ to 106 ± 16 nM ($n = 7$; $P < 0.05$) in the presence of 2 mM $[Ca^{2+}]_o$. The effect of store depletion on $[Ca^{2+}]_i$ baseline was further potentiated (to 305 ± 55 nM; $n = 8$; $P < 0.05$) by a fivefold increase of the driving force for Ca^{2+} entry. These data suggest that continuous Ca^{2+} entry in light-adapted rod photoreceptors is modulated by depletion of Ca^{2+} stores.

An alternative protocol for depleting Ca^{2+} stores in light-adapted rods employed sequential application of the ryanodine receptor agonist caffeine in Ca^{2+}-free saline. Repeated caffeine puffs evoked progressively lowered amplitude $[Ca^{2+}]_i$ transients due to emptying of ryanodine-sensitive stores. Re-exposure of store-depleted cells to 2 mM Ca^{2+} triggered a $[Ca^{2+}]_i$ overshoot of ~230 nM (Fig. 2*A*) Similar results were observed in 4/5 cells. Store depletion was also associated with transient increases in $[Ca^{2+}]_i$ in depolarized cells. In rods depolarized with 20 mM KCl, Ca^{2+} influx through L-type voltage-activated channels raised $[Ca^{2+}]_i$ to 300 nM. Under these conditions, 10 mM caffeine caused a large, rapid and transient Ca^{2+} release from ryanodine stores (Fig. 2*A*, inset). Release from stores was followed by prolonged undershoot marking store depletion and reduction in CICR, lowering baseline $[Ca^{2+}]_i$ by ~40%. The subsequent switch to caffeine-free control KCl-saline resulted in a secondary transient elevation of $[Ca^{2+}]_i$ in these depolarized, store-depleted rods (194 ± 39 nM; $n = 36$; no secondary elevation was detected in 9 rods) (Fig. 2*A*, inset; arrowhead). These data suggest that depletion of Ca^{2+} stores in both depolarized and hyperpolarized rod photoreceptors is associated with subsequent Ca^{2+} entry from extracellular saline.

The $[Ca^{2+}]_{IS}$ overshoots in response to store depletion resemble the so-called off-response representative of store-operated Ca^{2+} entry in non-excitable cells (Putney, 1990). Plasma membrane 'store-operated Ca^{2+} channels' (SOC channels) were recently shown to mediate similar $[Ca^{2+}]_i$ overshoots in excitable cells (Usachev & Thayer, 1999; Kachoei *et al.* 2006). SOC channels are typically studied with a 'depletion protocol' that consists of emptying Ca^{2+} stores in 0 Ca^{2+} saline supplemented with 1 μM thapsigargin (which depletes ER stores by irreversibly inhibiting SERCA-mediated Ca^{2+} sequestration) and followed by re-addition of control $[Ca^{2+}]_o$ (Putney, 1990). This experimental approach elicited substantial $[Ca^{2+}]_i$ overshoots in the large majority of rod ISs (281 ± 16 nM; $n = 45/59$; $P < 0.0001$ for the 45 cells; Fig. 2*B–F*). The amplitude of the overshoot exhibited exponential dependence on $[Ca^{2+}]_o$ (Fig. 2*E*; upper trace) with a half-maximal sensitivity that was similar to the sensitivity of $[Ca^{2+}]_i$ baseline to changes in $[Ca^{2+}]_o$ (Fig. 2*E*; lower trace; half maximum at 2.46 mM for overshoot and 2.11 mM $[Ca^{2+}]_o$ for baseline changes). After reaching the peak, $[Ca^{2+}]_i$ slowly declined, possibly due to Ca^{2+}-mediated inactivation of ion channels and slow up-regulation of Ca^{2+}-ATPases in the plasma membrane (Fig. 2*A* and *B*) (Bautista *et al.* 2002).

L-type channel agonist FPL 64176 and antagonist nifedipine had little effect on the amplitude of the depletion-induced overshoot (Fig. 2*Fa* and *c*), nor was there an effect of 100 μM Cd^{2+} ($P = 0.6097$; $n = 6$) (Fig. 2*Fd*). We considered the possibility that Ca^{2+} overshoots are modulated by Ca^{2+} entry through cGMP-gated Ca^{2+} channels expressed in ISs of salamander cones (e.g. Rieke & Schwartz, 1994). However, at 100 μM, the selective CNG channel antagonist L-*cis*-diltiazem had no effect on the overshoot (Fig. 2*Fb*), suggesting that neither high-voltage-operated or CNG channels contribute to the overshoot produced by depletion of Ca^{2+} stores.

While it is generally accepted that a single, highly specific inhibitor of SOC channels does not yet exist, there is a consensus that a block by low (μM) concentrations of lanthanides is diagnostic for SOC channels (Parekh & Putney, 2005). At 10 μM, both La^{3+} and Gd^{3+} significantly reduced the amplitude of the Ca^{2+} overshoot (La^{3+}: overshoot $= 58 \pm 18$ nM; $P < 0.001$; Gd^{3+}: overshoot $= 115 \pm 13$ nM; $P < 0.001$, $n = 6$ for each) (Fig. 3*A*). In addition to trivalent cations, the econazole SKF 96365 is commonly used to block store-operated Ca^{2+} influx. The amplitude of depletion-induced Ca^{2+} overshoots in rods was significantly reduced by 5 μM SKF 96365 (Fig. 3*A*; $n = 7$). The mean change in $[Ca^{2+}]_i$ after exposure to SKF 96365 was a 63% suppression, significantly different from cells treated with thapsigargin alone ($P < 0.05$). SKF 96365 suppressed the increase in thapsigargin-induced baseline $[Ca^{2+}]_i$ elevation in 2 mM and 10 mM $[Ca^{2+}]_o$ (see online supplemental material, Supplemental Fig. 1). The dihydropyridine MRS-1845 was recently shown to represent a selective high-affinity SOC channel antagonist (Harper *et al.* 2003). MRS-1845 alone had no effect on the amplitude or time course of depolarization-evoked $[Ca^{2+}]_i$ responses (Fig. 3*B*) or I_{Ca} (Fig. 5*B*), indicating it does not affect Ca^{2+} influx through L-type channels. MRS-1845 decreased the 30 mM KCl-evoked $[Ca^{2+}]_i$ signal to 96 ± 8% of the original response (from 1216 ± 257 control to 1055 ± 136 nM in the presence of MRS-1845, $P > 0.05$). However, MRS-1845 caused a significant decrease in the amplitude of SOCE (the overshoot in the presence of MRS-1845 was 94 ± 13 nM; $n = 7$; $P < 0.001$, Fig. 3*C*).

Taken together, the data presented in Figs 1–3 suggest that rod photoreceptors express a novel plasma

membrane Ca^{2+}-permeable pathway that exhibits the pharmacological profile characteristic of SOC channels. If these channels are activated by depletion of stores, the spatial profile of depletion-activated Ca^{2+} entry across the IS should reflect the local distribution of ER cisternae.

Ca^{2+} entry through SOCs is compartmentalized

The photoreceptor IS is polarized into distinct compartments specialized for aerobic metabolism (ellipsoid), gene expression (cell body) and synaptic transmission (synaptic terminal), respectively. Depolarization evokes $[Ca^{2+}]_i$ signals across IS regions that match the density of voltage-activated Ca^{2+} channels. Voltage-activated Ca^{2+} channels in the IS are expressed at high density in the synaptic terminal with a gradient of progressively lower density of voltage-activated Ca^{2+} channels towards the ellipsoid (Morgans *et al.* 1998). The $[Ca^{2+}]$ signature mediated by L-type channels in depolarized rods is characterized by at least two-fold higher signal amplitude in the synaptic terminal compared to the cell body (Szikra & Krizaj, 2006). In contrast, the SOCE pattern in the IS matches the distribution of ER cisternae rather than the distribution of L-type channels, cGMP-dependent channels or mitochondria (Fig. 4) (e.g. Rieke & Schwartz, 1994, 1996; Szikra & Krizaj, 2007). The amplitude of depletion-induced Ca^{2+} overshoots in the synaptic terminal (253 ± 31 nM, $n = 4$; arrowhead in Fig. 4) was slightly, but not significantly, lower than the amplitude of SOCE measured in cell body (281 ± 16 nM; black trace); SOCE amplitudes were approximately halved in the ellipsoid region (141 ± 22 nM, $n = 9$; $P < 0.001$) (Fig. 4, grey trace).

These data suggests that cytosolic $[Ca^{2+}]_i$ levels regulated by voltage-operated *versus* store-operated Ca^{2+}-permeable channels reach different absolute concentrations during maximal activation across IS compartments. Whereas the amplitude of depolarization-evoked responses shows a marked gradient from the terminal towards the ellipsoid (Szikra & Krizaj, 2006), the store-operated signals show similar amplitudes in the perikaryon and the terminal, indicating differential expression of voltage- and store-operated channels.

Ca^{2+} entry through SOCs modulates exocytosis

Ca^{2+}-dependent exocytosis in rod terminals is strongly regulated by Ca^{2+} release from ryanodine stores (Suryanarayanan & Slaughter, 2006; Cadetti *et al.* 2006). It is not clear whether Ca^{2+} is released from stores within the terminal itself or whether it reaches active sites via diffusion from perinuclear storage sites in the cell body. We first investigated the predicted location of releasable Ca^{2+} stores in rod terminals and ascertained whether store depletion of terminals triggers SOCE and regulates exocytosis.

To determine whether rod terminals contain releasable Ca^{2+} stores, store content of untreated cells was released with the Ca^{2+} ionophore ionomycin in Ca^{2+}-free saline. Ionomycin triggered transient release of Ca^{2+} from intracellular stores in the synaptic terminal (1133 ± 410 nM, $n = 3$ rod terminals, Fig. 5*A*, black trace). This release occurred in the absence of Ca^{2+} influx from the extracellular space, indicating that salamander spherules store significant amounts of Ca^{2+}. The store depletion protocol was repeated on rod terminals. As illustrated in Fig. 5*B* and *C* (also see Fig. 4*A*), marked SOCE was observed in rod terminals with depleted Ca^{2+} stores. Although SOCE amplitude was low compared to $[Ca^{2+}]_i$ signals mediated by L-type channels upon depolarization (which probably saturated the fura-2 signal; Fig. 5*C*), these data suggest that endogenous SOC channels may contribute to reloading of synaptic Ca^{2+} stores in hyperpolarized rods.

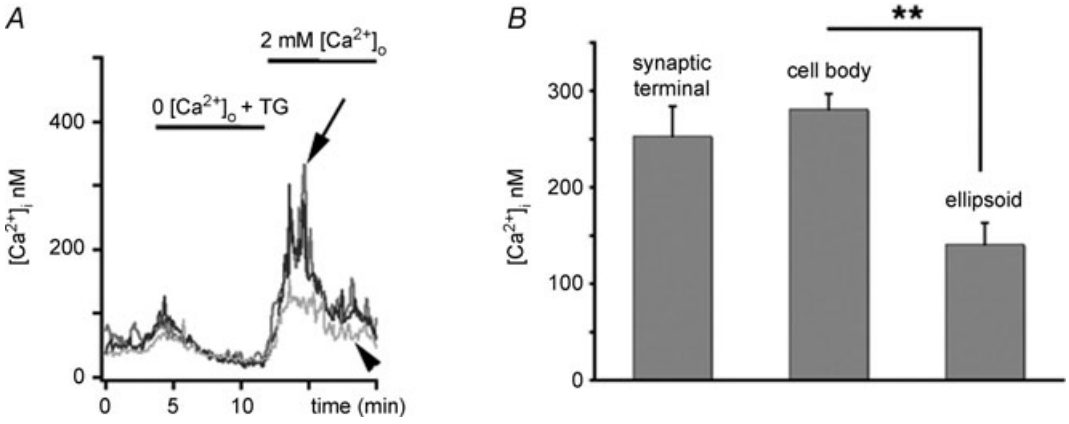

Figure 4. Compartmentalization of SOCE in rods
A, depletion-evoked $[Ca^{2+}]_i$ overshoots had similar amplitudes in the cell body (black trace) and in the synaptic terminal (grey trace, arrow), with slightly lower elevations in the ellipsoid region (light grey, trace, arrowhead). *B*, data summary for each IS compartment.

To test whether store-operated Ca^{2+} entry could mobilize fusion-competent synaptic vesicles, isolated retinas were incubated with the membrane dye FM1–43 (5 μM). Isolated rods were superfused with 0 Ca^{2+} saline containing 1 μM thapsigargin to block exocytosis and deplete internal stores. Re-exposure to 2 mM $[Ca^{2+}]_o$ saline induced significant destaining of labelled terminals (Fig. 5*D*). In six terminals, the destaining over 3 min was $56 \pm 9\%$. In non-synaptic regions such as the cell body, the destaining was significantly less ($17 \pm 9\%$), probably due to residual dye bleaching and/or partial retraction of the terminal into the cell body. Activation of voltage-operated Ca^{2+} channels significantly increased the amplitude and kinetics of FM1–43 compared to SOCE-mediated signals (Fig. 5*E*; $n = 7$; $P < 0.05$), consistent with the dominant role for voltage-operated Ca^{2+} entry in the control of vesicle release at rod synapses (Thoreson *et al.* 2004).

SOC channels modulate rod neurotransmission

To test whether SOC channels localized to the synaptic terminal modulate synaptic transmission, light responses were recorded from current-clamped rods and voltage clamped horizontal cells in the presence of the SOC channel antagonist MRS-1845. Bath application of MRS-1845 (15 μM) for 3 min had no effect on the rod light response evoked by 580 nm illumination (test/control $= 1.04 \pm 0.06$, $n = 3$, Fig. 6*A*) nor did it affect voltage-activated Ca^{2+} currents measured in voltage clamped rods using a voltage ramp protocol (0.98 ± 0.04, $n = 7$, Fig. 6*B*). In contrast, the SOC channel antagonist reduced the magnitude of light-evoked currents in horizontal cells by $20 \pm 9\%$ ($n = 15$; $P < 0.05$) (Fig. 6*C*). MRS1845 also caused an outward baseline shift in the membrane currents of horizontal cells in darkness ($+51.3 \pm 15.1$ pA, $n = 15$, $P = 0.004$) consistent with a reduction in the maintained release of glutamate from rods in darkness. (A baseline shift of +46 pA was removed from Fig. 6*C* to facilitate comparison of light response waveforms.) We also tested the effects of bath applying MRS-1845 on synaptic transmission in simultaneously recorded pairs of rods and horizontal cells. A postsynaptic current was evoked in a horizontal cell by applying a strong depolarizing test step to a simultaneously recorded rod. The test step from −70 to −10 mV was designed to stimulate maximal release (Thoreson *et al.* 2004; Cadetti *et al.* 2005). As illustrated in Fig. 6*D*, depolarization of a rod evoked an initial transient inward postsynaptic current in the horizontal cell followed by a sustained inward current that subsided to baseline soon after the depolarizing stimulus was terminated. MRS-1845 had no effect on the initial fast inward synaptic current consistent with other findings suggesting that the initial burst of depolarization-evoked release results largely from the opening of calcium channels (Cadetti *et al.* 2005, 2006). Light-evoked currents involve changes in sustained synaptic release and, consistent with a role for SOC channels in modulating sustained release, MRS-1845 produced a reversible reduction in the slower sustained component of the rod-driven synaptic current (Figs 6*D*, $n = 4$). These data suggest SOC channels can modulate sustained neurotransmitter release from rods.

TRPC channels are localized to salamander photoreceptors

Molecular cloning, heterologous expression and antisense studies have implicated the seven vertebrate homologues of the *Drosophila* light-sensitive TRP channel as endogenous plasma membrane channels in mediation of

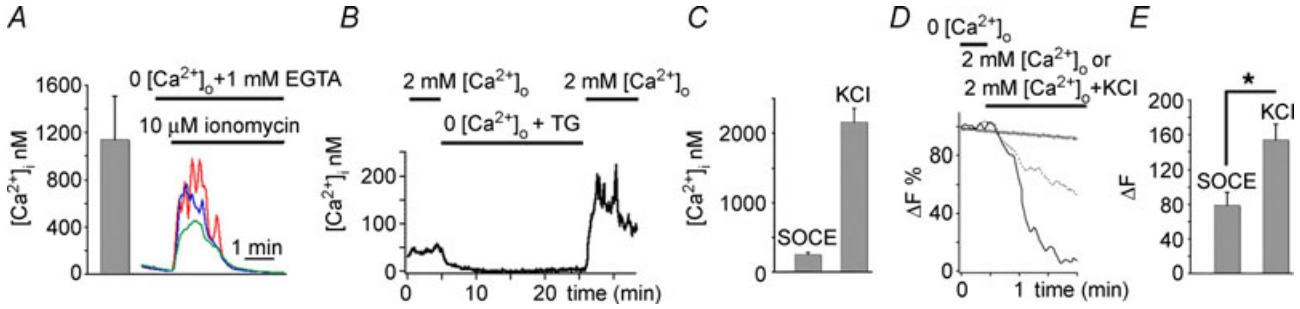

Figure 5. SOCE in synaptic terminal modulates exocytosis
A, rod terminals store Ca^{2+} in intracellular stores. Rod terminal superfused with 0 Ca^{2+} saline was exposed to 10 μM ionomycin. The ionophore released free Ca^{2+} from an internal reservoir. *B*, store depletion with 1 μM thapsigargin in 0 Ca^{2+} saline evokes SOCE in a rod terminal. *C*, the amplitude of maximal SOCE compared to $[Ca^{2+}]_i$ amplitudes obtained from activation of Ca^{2+} entry through L-type Ca^{2+} and ryanodine-receptor channels in cells depolarized with 30 mM KCl. *D*, cells stained with the activity-dependent dye FM1–43 (5 μM). ROI placed on the terminal and cell body regions of the IS. The depletion protocol induced a significant destaining in the synaptic terminal (dotted trace) and less destaining in the cell body (open circle). The amplitude and rate of depletion-evoked destaining was less that destaining induced by 30 mM KCl (continuous trace). *E*, data summary for exocytosis induced by SOCE and depolarization.

depletion-evoked plasma membrane Ca^{2+} fluxes (Zhu *et al.* 1996; Wu *et al.* 2004; Liu *et al.* 2007), acting in association with STIM1 and Orai1 proteins (Chen *et al.* 2008). Hence, immunostaining, RNAi transfection and Ca^{2+} imaging were used to determine the expression of canonical transient potential receptor channels (TRPCs) in the retina and their role in photoreceptor SOCE.

TRPC localization. Immunostaining of vertical retinal sections with antibodies against TRPC channel isoforms 1 and 6 showed prominent immunoreactivity in the outer retina. TRPC1 signals were predominantly localized to rods, with prominent labelling of the subellipsoid region that contains most of rod ER (Fig. 7*Ab* and *c*; *Ba* and *b*). The ellipsoid was weakly labelled, with most signal concentrated in the plasma membrane surrounding this IS region whereas the cell body and the synaptic terminal were moderately stained, as was the proximal part of the outer segment. Two different TRPC1 antibodies were used in these experiments. While the two antibodies showed a similar overall immunostaining pattern, one antibody (Chemicon/Millipore) labelled the proximal OS (Fig. 7*A*), whereas OS labelling was absent from the second antibody (Sigma; Fig. 7*B*). No TRPC1 signal was detected in the absence of primary antibodies (data not shown) or following co-incubation with specific neutralizing peptides derived from the cytoplasmic, NH_3-terminal domain of the TRPC1 (Fig. 7*Ad*). Double labelling with the synaptic vesicle marker SV2 showed partial colocalization with TRPC1 in the OPL, consistent with TRPC1 expression in a subset of OPL synapses. In contrast to TRPC1 immunolabelling, the TRPC6 antibody predominantly labelled cone perikarya and synaptic terminals (Fig. 7*B*). At higher confocal gains, TRPC6 immunostaining was typically observed in distinct

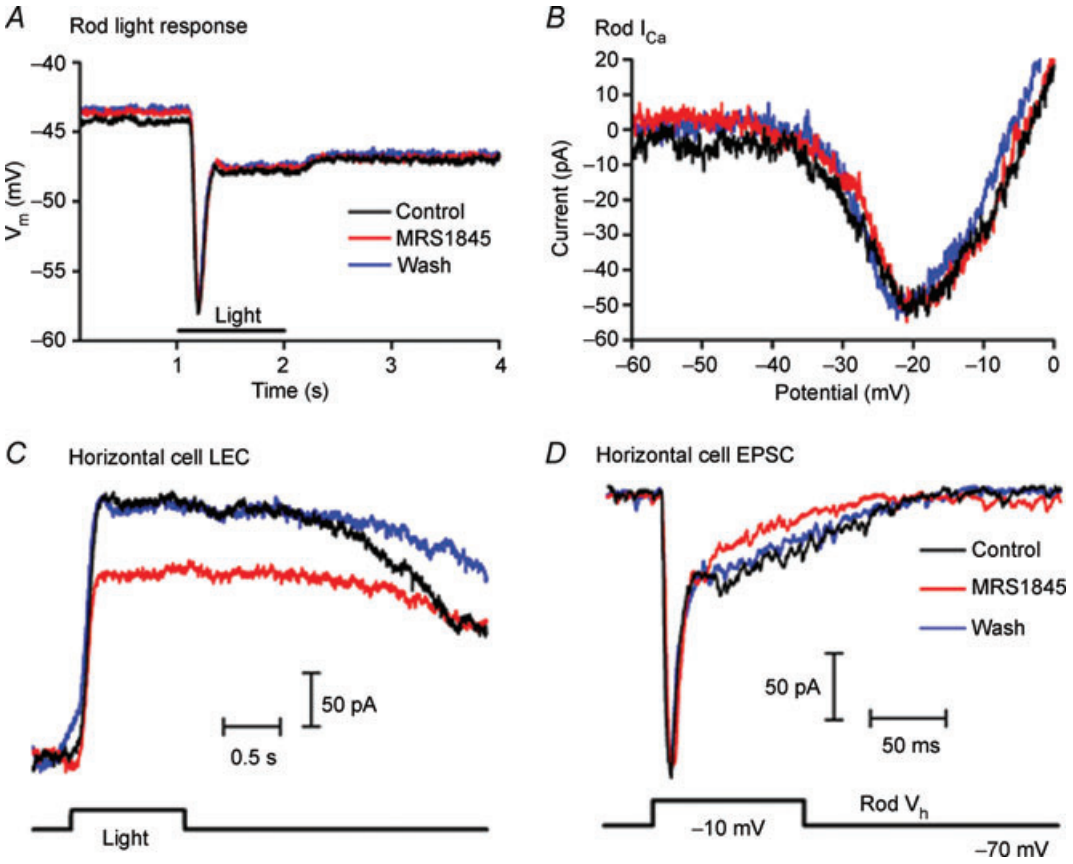

Figure 6. SOC channels modulate rod neurotransmission
A and *B*, the SOC channel antagonist MRS-1845 (15 μM) had no effect on the rod light response evoked by 1 s 580 nm flash (*A*) or I_{Ca} evoked by depolarizing ramps (−90 to +50 mV, 0.5 mV ms^{-1}) (*B*). *C*, light-evoked current recorded from a horizontal cell was significantly reduced in the presence of MRS-1845. MRS-1845 also caused an outward shift of 46 pA in the horizontal cell membrane current in darkness that was removed for comparison of light response waveforms. *D*, in a simultaneously recorded rod and horizontal cell pair, depolarizing the presynaptic rod to −10 mV for 100 ms evoked both transient fast and sustained slow EPSC components in the horizontal cell. MRS-1845 selectively decreased the sustained EPSC component. In all experiments illustrated in this figure, MRS-1845 was bath applied for 3–4 min.

puncta within the inner retina (Fig. 7*Bb*). TRPC6 signals were not observed in the absence of the primary antibody (not shown) or following co-incubation with specific neutralizing peptides (Fig. 7*Cd*). Taken together, these data suggest that TRPC channel isoforms in salamander retinal neurons are expressed in a cell type-specific manner.

Elimination of TRPC1 reduces depletion-evoked signals in rods, but not cones

Although electrophysiological recordings and immunostaining indicate that amphibian tissues express several different TRPC isoforms (Wang & Poo, 2005), the amphibian TRPC1 homologue xTRP-1 is the only isoform

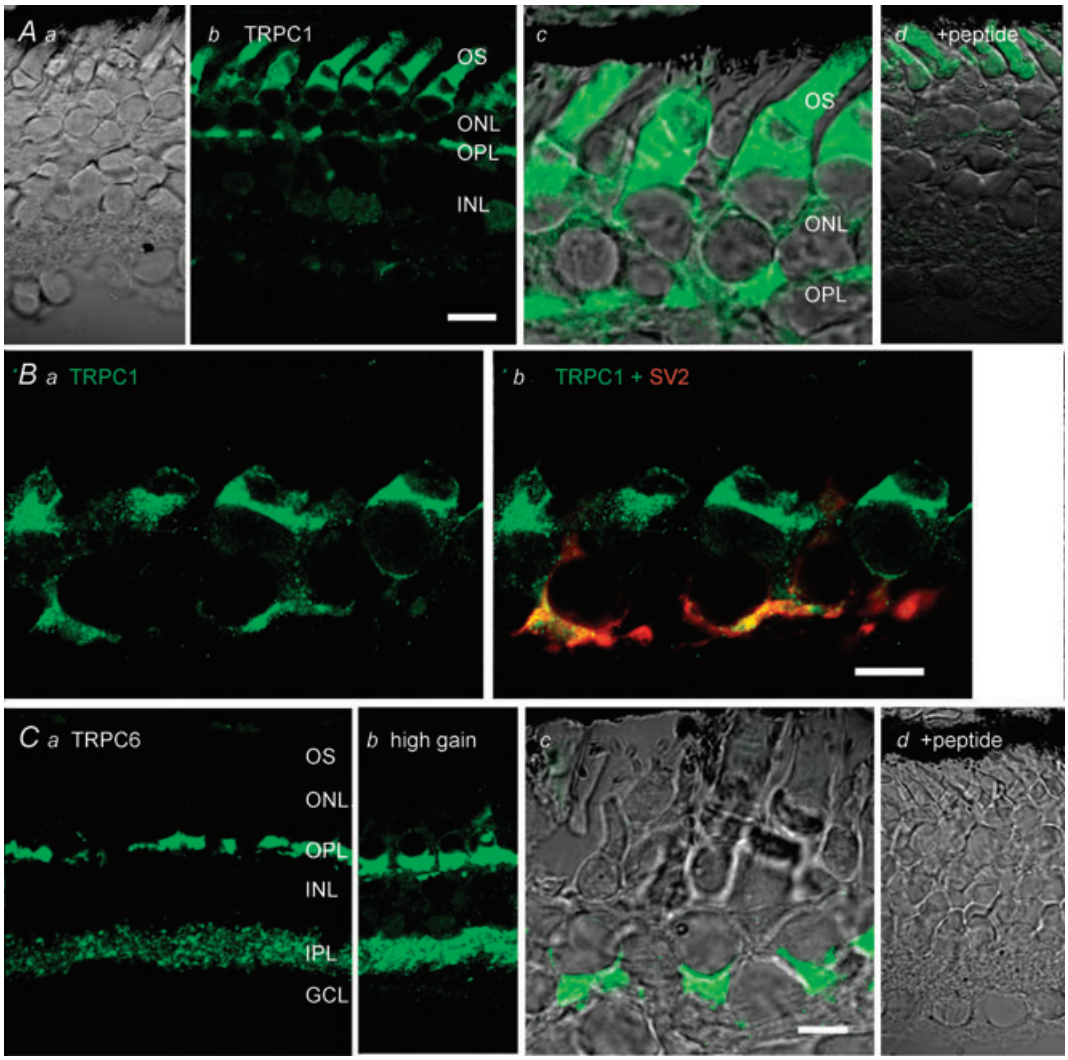

Figure 7. Localization of TRPC channel isoforms in salamander retina
Aa, DIC image of a transverse retinal section. *Ab*, immunostaining for TRPC1 with the Millipore antibody. *Ac*, TRPC1 signal is localized to the cell body and synaptic regions of rods; subellipsoid, ellipsoid and proximal OS domains are also labelled by the antibody. *Ad*, DIC + fluorescence. No signal is observed in the presence of equal concentration of the neutralizing peptide. *B*, immunostaining for TRPC1 with the Sigma antibody, colocalization with SV2. *Ba*, the antibody labels cell bodies and synaptic terminals of rods; the signal is absent from the OS. Strong labelling is observed in the subellipsoid region and in plasma membrane surrounding the ellipsoid. *Bb*, colocalization of TRPC1 and SV2 immunoreactivity in rod terminals. *C*, immunostaining for TRPC6. *Ca*, cone cell bodies and synaptic terminals are labelled; fluorescent puncta are observed in the IPL. *Cb*, TRPC6 immunoreactivity at high confocal gain shows labelling in the cone cell body and potential labelling in rod terminals proximal to cone pedicles. *Cc*, DIC + fluorescence inset from the outer retina; *Cd,* DIC + fluorescence in presence of the neutralizing peptide. Abbreviations: OS, outer segment; IS, inner segment; ONL, outer nuclear layer; OPL, outer plexiform layer; INL, inner nuclear layer; IPL, inner plexiform layer; GCL, ganglion cell layer. Scale bar = 20 μm in *Aa*, *b* and *d* and *Ca–d*; 10 μm in *Ac*, *B* and *Cc*.

so far cloned (Bobanovic *et al.* 1999; Brereton *et al.* 2000). An RNAi sequence based on xTRP-1 was designed to silence the TRPC1 isoform in salamander retinas. Isolated retinas were incubated with 200 nM xTRP1 or control RNAi for 24 or 48 h. Subsequently, the retinas were homogenized for protein analysis or dissociated and loaded with the calcium indicator dye fura-2. Because TRPC1 antibodies that labelled rods with the immunostaining technique did not recognize any epitopes in immunoblotted amphibian tissue ($n = 3$ separate experiments) we used mouse polyclonal antibodies raised against xTRP-1 (a generous gift from Dr Leonidas Tsiokas, University of Oklahoma Health Sciences Center). Immunoblots showed a band at ~70 kDa, close to the molecular mass of the amphibian xTRP1 (Bobanovic *et al.* 1999) that was absent from RNAi-treated retinas (Fig. 8*A*), suggesting that RNAi incubation had an inhibitory effect on expression/stability of the TRPC1 protein. A weak protein band in gels from RNAi-treated retinas is reflected in weaker retinal staining with the TRPC1 antibody (Sigma) (Fig. 8*B*). Compared with the vehicle (transfection reagent), 24–48 h targeting with xTRP1 RNAi yielded a 40–50% suppression of depletion-evoked $[Ca^{2+}]_i$ overshoots in rod cell bodies (Fig. 8*C*). In contrast, simultaneously imaged cones exposed to the identical transfection protocol showed no significant effect with xTRP1 (Fig. 8*D*). Exposure of rods to the transfecting agent alone or the presence of a non-silencing RNAi control sequence had no effect on the amplitude of depletion-evoked $[Ca^{2+}]_i$ overshoots or on viability of the cells (24 h incubation, rods/cones: $n = 10/14$ and $n = 9/11$ for control and RNAi treated, respectively; 48 h incubation: $n = 7/9$ and $n = 5/10$ for control and RNAi treated, respectively; $P < 0.05$ between control and treated rods; Fig. 8*C* and *D*. At 48 h, non-silencing RNAi alone had no effect on SOCE in rods or cones ($n = 11/14$). These results are consistent with the idea that TRPC1 is an essential component of store-operated Ca^{2+} entry in rods, but not cones.

Discussion

The present study shows that vertebrate rods express a novel plasma membrane Ca^{2+} influx pathway that carries the biochemical, pharmacological and physiological signature of SOCE. This store depletion-sensitive influx mechanism contributes significantly to Ca^{2+} homeostasis in the rod IS and modulates neurotransmission at the rod synapse.

Store-operated Ca^{2+} entry modulates baseline $[Ca^{2+}]_i$ in light-adapted cells

We found that $[Ca^{2+}]_i$ in light-adapted rod ISs is sensitive to changes in the Ca^{2+} driving force. A fivefold increase in $[Ca^{2+}]_o$ led to a doubling of the concentration of free Ca^{2+} within the IS through a sustained Ca^{2+} influx mechanism. This pathway contributed a significant fraction of baseline $[Ca^{2+}]_i$ in light-adapted cells (~26 nM, i.e. ~60% of total free cytosolic $[Ca^{2+}]$). Similar $[Ca^{2+}]_i$ dependence on $[Ca^{2+}]_o$ was previously attributed to modulation of Ca^{2+} release from neuronal stores and plasma membrane Ca^{2+} transport (Nohmi *et al.* 1992; Gomez *et al.* 1995). However, $[Ca^{2+}]_o$-induced changes in $[Ca^{2+}]_i$ were in the opposite direction from that expected by modulation of surface charges associated with the rod plasma membrane (i.e. an increase in $[Ca^{2+}]_o$ would be expected to decrease $[Ca^{2+}]_i$ by shifting the activation of the L-type channel in the hyperpolarizing direction; Baldridge *et al.* 1998), suggesting they were not mediated by voltage-activated Ca^{2+} channels. Consistent with this interpretation, $[Ca^{2+}]_o$-induced Ca^{2+} influx across the

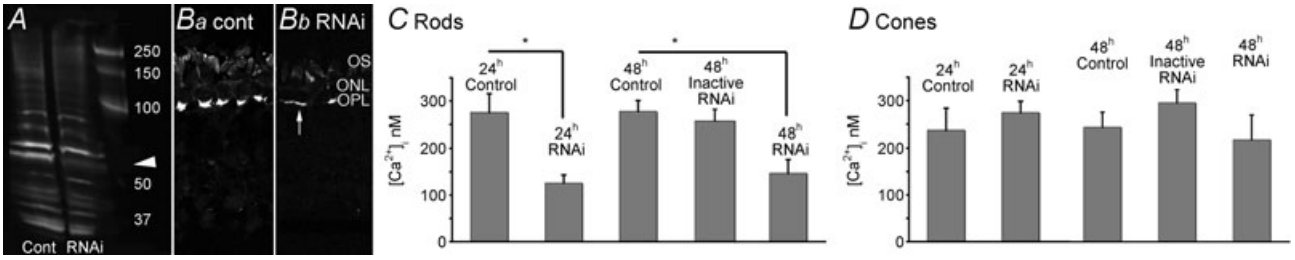

Figure 8. xTRP1 RNAi suppresses SOCE in rods but not cones
A, TRPC1 immunoblots from control and RNAi-treated retinas. The transfected retina shows a decrease in a ~70 kDa band corresponding to TRPC1; *B*, immunostaining of control (*Ba*) and RNAi-treated retinas with the TRPC1 antibody shows a reduction in the RNAi signal. The staining was confined to narrow stripe within the OPL (arrow in *Bb*). *C*, Ca^{2+} imaging of depletion-evoked signals from control (transfecting reagent only), rods incubated with the 'Silencer' control RNAi and xTRP1 RNAi- transfected rod ISs at 24 h and 48 h incubation. Cells were loaded with 5 μM fura-2 AM and their stores depleted in 0 Ca^{2+} + thapsigargin. Bar graph amplitudes denote peak Ca^{2+} overshoots following return to control saline. *D*, Ca^{2+} imaging from ISs of control, 'Silencer' control RNAi and xTRP1 RNAi-transfected fura 2-loaded cones at 24 h and 48 h incubation. No significant differences were observed in cones from control, 'Silencer'-treated or transfected retinas.

rod IS plasma membrane was insensitive to L-type and CNG channel agonists and antagonists; it was, however, potentiated by depletion of internal Ca^{2+} stores with ryanodine receptor agonists and by irreversible inhibition of SERCA-mediated Ca^{2+} sequestration. Comparable elevations in $[Ca^{2+}]_i$ were observed previously following direct inhibition of SERCA transporters (Krizaj *et al.* 2003), suggesting that the prime function of this Ca^{2+} entry pathway is to refill internal Ca^{2+} stores. The observation that store depletion elevated $[Ca^{2+}]_i$ only in the presence of millimolar $[Ca^{2+}]_o$ suggests that it activates a plasma membrane, rather than a cytoplasmic, Ca^{2+} channel.

Although SOCE is universally accepted as the major Ca^{2+} entry mechanism in non-excitable cells, concrete evidence for its existence and physiological relevance in excitable cells has been more difficult to demonstrate mainly due to technical difficulties associated with measurement of low-amplitude transmembrane currents (Parekh & Putney, 2005). Instead, indirect approaches such as fura-2 measurements of cytoplasmic calcium are generally used to show that store depletion modulates $[Ca^{2+}]_i$ in muscle cells and neurons (Hopf *et al.* 1996; Fomina & Nowycky 1999; Bouron *et al.* 2004; Kachoei *et al.* 2006; Prakash *et al.* 2006). Endogenous SOC channels are typically identified by their sensitivity to micromolar concentrations of lanthanides and organic SOCE antagonists such as SKF-96365, 2-APB and MRS-1845. The pharmacological profile of sustained Ca^{2+} influx in light-adapted rod ISs – (a) suppression by 1 μM La^{3+} and Gd^{3+}, (b) suppression by MRS-1845, 2-APB and SKF 96365, (c) insensitivity to modulators of L-type and CNG channels, and (d) facilitation by depletion of ER stores – strongly matches that of SOCE. The sensitivity of depletion-evoked signals to lanthanides and thapsigargin further suggests that these plasma membrane channels do not belong to non-store or receptor-activated cation channels that are often activated in parallel to SOCE (Smyth *et al.* 2006). Taken together, the pharmacological profile of Ca^{2+} entry at resting (hyperpolarized) membrane potentials and depletion-mediated Ca^{2+} influx suggest that vertebrate rods express a Ca^{2+} influx pathway that corresponds to SOCE. Hence, our results suggest that $[Ca^{2+}]_i$ in light-adapted rod ISs reflects a homeostatic balance between Ca^{2+} channels represented by SOC channels and PMCA-mediated Ca^{2+} extrusion, SERCA2-mediated Ca^{2+} sequestration and mitochondrial Ca^{2+} buffering (e.g. Krizaj *et al.* 2003; Szikra & Krizaj, 2007). Na^+/Ca^{2+} exchange is absent from amphibian rod ISs (Krizaj & Copenhagen, 1998), but it could play a more significant role in modulation of baseline $[Ca^{2+}]_{IS}$ in mammalian cones (e.g. Johnson *et al.* 2007).

The main effect of store depletion in rod ISs was a potentiation of Ca^{2+} influx into the rod IS cell body, with lesser signals in the synaptic terminal and ellipsoid regions. This spatial pattern matches both distribution of ER cisternae (Mercurio & Holtzman, 1982) and the spatial pattern of rod $[Ca^{2+}]_i$ triggered by ryanodine receptor agonist caffeine (Krizaj *et al.* 2003), but is dissimilar from the pattern induced by activation of voltage-operated Ca^{2+} channels or mitochondrial Ca^{2+} signalling (Rieke & Schwartz, 1996; Cadetti *et al.* 2006; Szikra & Krizaj, 2007), further consistent with feedback interaction between plasma membrane Ca^{2+}-permeable channels and the ER.

TRPC1 is required for store-operated Ca^{2+} entry in rods

TRPC1 is a cation channel highly conserved across mammals, amphibians and birds (Ambudkar, 2007). In the avian retina, TRPC1 immunoreactivity was detected across several cell types in the inner retina (Crousillac *et al.* 2003). Cation entry through TRPC1 channels is antagonized by 10 μM Gd^{3+} (Zitt *et al.* 1996), 100 μM 2-APB (Zagranichnaya *et al.* 2005) and 10 μM SKF96365, consistent with the pharmacological characteristics of rod SOCE (Fig. 2). In salamander, TRPC1 antibodies predominantly labelled rod photoreceptors, with the signal localized mainly to the IS and synaptic terminal. Surprisingly, one TRPC1 antibody produced a modest signal in the proximal OS, possibly matching the distribution of ryanodine receptors within the OS (Shoshan-Barmatz *et al.* 2007); however, another antibody raised against the same epitope labelled the same photoreceptor compartments but did not stain the OS (Fig. 7*B*), and hence potential expression of TRPC1 in the OS remains to be determined in future studies. To ascertain the TRPC1 role in photoreceptor IS calcium signalling, we targeted the amphibian xTRP channel, the sequence of which corresponds to the mammalian TRPC1 (Bobanovic *et al.* 1999; Brereton *et al.* 2000; Wang & Poo, 2005). xTRP1 representing the sole TRPC homologue cloned so far in amphibians shows 81% identity and 90% similarity in amino acid structure to the mammalian TRPC1 (Bobanovic *et al.* 1999). Targeting of the xTRP1 gene using a RNAi sequence generated against a 12 amino acid domain of the amphibian xTRP1 selectively reduced the expression of the endogenous protein in the transfected retina and the amplitude of depletion-evoked $[Ca^{2+}]_i$ signals in transfected rods. SOCE was unaffected by a control 'silencer' RNAi sequence. In contrast to rods, cone IS responses were unaffected by xTRP1 RNAi, consistent with absence of TRPC1 immunoreactivity from cones. Unchanged $[Ca^{2+}]_i$ responses in cones dissociated from transfected retinas also suggest that the transfection procedure itself did not cause a non-specific suppression of transcription. Interestingly, the residual TRPC1 signal in RNAi-treated retinas appeared to be confined to a thin stripe within the OPL, suggesting a potential remodelling of rod terminals and/or TRPC1 mislocalization (Fig. 8*Bb*).

While our data suggests that TRPC1 represents a signalling element in communication between Ca^{2+} stores and the plasma membrane, the mechanism whereby rod ER stores interact with TRPC1 channels remains for further study. Inhibition of store-operated signals in salamander rods by antagonists that typically suppress Ca^{2+} entry through SOC, Orai1, TRPC and/or xTRP channels, together with the observation that not all SOCE was blocked by TRPC1 knockdown, allows for different combinations of ER–plasma membrane transduction mechanisms. Despite abundant experimental evidence showing TRPC1 as a candidate SOC channel (Beech, 2005; Ambudkar, 2007), a number of other studies show that TRPC1 forms receptor-operated channels (ROCs) that are insensitive to store depletion (Parekh & Putney, 2005). It is possible that retinal TRPC1 channels form both ROC and SOC channels, depending on localization and expression of the stromal interaction protein (STIM1) (Liao *et al.* 2007; Yuan *et al.* 2007; Alicia *et al.* 2008). Whereas coexpression of Orai1 and STIM1 generates currents that resemble the paradigmatic CRAC channel in lymphocytes (Lewis, 2007; Zhang *et al.* 2008) and SOCE is inhibited in Orai1 knockout mice (Vig *et al.* 2008), the TRPC1 protein was clearly shown to mediate SOCE in heterologously expressing systems as well as to represent endogenous SOC channels in several types of tissue, including excitable cells (Wu *et al.* 2004; Ambudkar, 2007; Worley *et al.* 2007). TRPC1 forms functional SOC channels when coexpressed with STIM1 (Liao *et al.* 2007; Yuan *et al.* 2007) and SOCE is clearly compromised in TRPC1 knockout animals (Liu *et al.* 2007), consistent with our observation that SOCE in rod photoreceptors is decreased following TRPC1 knockdown. Both TRPC and Orai channels are regulated by STIM1 (Soboloff *et al.* 2006; Yuan *et al.* 2007) and we cannot exclude the possibility that SOCE in rod ISs is regulated by coactivation of endogenous Orai1, STIM1 and TRPC1 protein complexes (e.g. Ong *et al.* 2007; Cheng *et al.* 2008). The remaining depletion-evoked signal in xTRP1 RNAi-treated rods could therefore have been mediated by endogenous Orai1 channels activated by accumulation of depletion-induced STIM1 aggregates underneath the plasma membrane or by other TRP isoforms expressed in rod ISs. Retinal expression or localization of Orai1 proteins is currently not known, but localization of Orai1 gene expression in some brain regions suggests that CRAC currents may be expressed within some types of excitable cell (Vig *et al.* 2008).

Store-operated Ca^{2+} entry in the synaptic terminal modulates exocytosis

Schmitz & Witkovsky (1996) discovered that a significant fraction of glutamate release in amphibian photoreceptors was not blocked by saturating white light expected to completely close rod voltage-operated Ca^{2+} channels. In contrast to light stimuli, KCl-evoked increases in exocytosis were completely suppressed by L-type channel antagonists (Schmitz & Witkovsky, 1997), suggesting that light-sensitive exocytosis from amphibian rods could be modulated by other, voltage-independent pathway(s) perhaps similar to cGMP-dependent mechanisms in cone terminals (Rieke & Schwartz, 1994). While Ca^{2+} influx into hyperpolarized rods was unaffected by inhibitors of cGMP-gated channels, both Ca^{2+} and synaptic signals were affected by modulation of SOCE. The SOC channel antagonist MRS-1845 inhibited sustained synaptic release from rods to postsynaptic horizontal cells (Fig. 6). The observation that depletion of Ca^{2+} stores directly stimulates presynaptic vesicle release (Fig. 5*D*) and that MRS-1845 potently suppresses SOCE in isolated rods (Fig. 2) while having no effect on the rod light response, I_{Ca} or depolarization-evoked $[Ca^{2+}]_i$ elevations in the rod IS, militates against the hypothesis that MRS-1845 simply affects signalling in the postsynaptic cell. Indeed, the rate of depletion-induced destaining in FM1–43-loaded terminals was similar to rates previously observed in intact retinas (Choi *et al.* 2005). Similarly, a previous capacitance study in chromaffin cells directly ascertained that SOCE plays a significant role in exocytosis (Fomina & Nowicky, 1999). The contribution of SOC channels to exocytosis in rod photoreceptors may have been overlooked in previous studies because maximal store-operated $[Ca^{2+}]_i$ signals rarely exceed 200–300 nM (close to the exocytosis threshold for rods; Thoreson *et al.* 2004); in capacitance studies (Rieke & Schwartz, 1996; Kreft *et al.* 2003; Thoreson *et al.* 2004), the low release rate mediated by SOCE was likely compensated for in the measurement of baseline capacitance.

Physiological significance of calcium stores and SOCE for the function of vertebrate rods

SOCE serves to replenish ER stores in hyperpolarized IS compartments from which cytosolic Ca^{2+} ions are continually extruded via powerful ATPase pumps. Similar to the proposed role for cGMP-mediated Ca^{2+} influx into salamander cones (Rieke & Schwartz, 1994), Ca^{2+} influx through presynaptic rod SOC channels could extend the operating range of rod synapses by increasing presynaptic $[Ca^{2+}]_i$ at higher light levels when influx through L-type Ca^{2+} channels is suppressed or blocked. These results complement recent studies documenting the essential role for rod Ca^{2+} stores at low light levels at which Ca^{2+} release is indispensable for maintaining sustained exocytosis (Suryanarayanan & Slaughter, 2006; Cadetti *et al.* 2006). Similar to effects of the SOC antagonist MRS-1845, inhibition of Ca^{2+}-induced Ca^{2+} release (CICR) had little effect on the initial fast component of synaptic currents evoked in horizontal cells by strong

depolarizing steps applied to rods (Suryanarayanan & Slaughter, 2006; Cadetti *et al.* 2006). Together, these results suggest that the initial burst of release evoked by strong depolarization is controlled mainly by the opening of Ca^{2+} channels. Despite minimal effects on the initial burst of release, blocking SOC channels or CICR inhibited slow, sustained synaptic currents of horizontal cells evoked by maintained depolarization of rods. Blocking SOC channels or CICR also inhibited light-evoked currents in horizontal cells suggesting that the regulation of intra-terminal calcium levels by Ca^{2+} stores is particularly important in maintaining the sustained release of vesicles that shapes the responses of second order retinal neurons in light and dark.

The present results further extend our understanding of signalling pathways that regulate Ca^{2+} homeostasis, and possibly dysfunction, in vertebrate rods. Given that the TRPC1 channel is known to be involved in growth cone path-finding (Wang & Poo, 2005; Shim *et al.* 2005), it will be of interest to determine whether rod TRP channels contribute to the extension of neurites with vesicle-laden synaptic varicosities towards the inner retina observed in a number of retinal degenerations (e.g. retinitis pigmentosa, age-related macular degeneration and retinal detachment) (e.g. Jones *et al.* 2005). Prolonged depletion of ER triggers large-scale apoptosis of rods (Chiarini *et al.* 2003) through disturbed gene expression, protein synthesis, and global suppression of mRNA translation (Bian *et al.* 1997; Lin *et al.* 2007, 2008). An important function of TRPC channels and SOCE may therefore be to protect cells by maintaining ER Ca^{2+} stores via specific stimulation of Ca^{2+}-sensitive signalling pathways within the IS (e.g. Jia *et al.* 2007). Taken together, these various pieces of evidence point at Ca^{2+} stores as an important hub involved in the generation and modulation of steady-state $[Ca^{2+}]_i$ within the rod inner segment as well as photoreceptor output signals.

In conclusion, our study emphasizes that a novel Ca^{2+} influx pathway activated by depletion of intracellular Ca^{2+} stores modulates the visual signal at the first synapse in the rod system. This pathway involves interactions between plasma membrane Ca^{2+}-permeable channels and ER stores, which appear to play a central role in sustaining tonic signalling at a tonic visual synapse.

References

Alicia S, Angélica Z, Carlos S, Alfonso S & Vaca L (2008). STIM1 converts TRPC1 from a receptor-operated to a store-operated channel: Moving TRPC1 in and out of lipid rafts. *Cell Calcium* (in press).

Ambudkar IS (2007). TRPC1: a core component of store-operated calcium channels. *Biochem Soc Trans* **35**, 96–100.

Bader CR, Bertrand D & Schwartz EA (1982). Voltage-activated and calcium-activated currents studied in solitary rod inner segments from the salamander retina. *J Physiol* **331**, 253–284.

Baldridge WH, Kurennyi DE & Barnes S (1998). Calcium-sensitive calcium influx in photoreceptor inner segments. *J Neurophysiol* **79**, 3012–3018.

Bautista DM, Hoth M & Lewis RS (2002). Enhancement of calcium signalling dynamics and stability by delayed modulation of the plasma-membrane calcium-ATPase in human T cells. *J Physiol* **541**, 877–894.

Beech DJ (2005). TRPC1: store-operated channel and more. *Pflugers Arch* **451**, 53–60.

Bian X, Hughes FM, Huang Y, Cidlowski JA & Putney JW Jr (1997). Roles of cytoplasmic Ca^{2+} and intracellular Ca^{2+} stores in induction and suppression of apoptosis in S49 cells. *Am J Physiol Cell Physiol* **272**, C1241–C1249.

Bobanovic LK, Laine M, Petersen CC, Bennett DL, Berridge MJ, Lipp P, Ripley SJ & Bootman MD (1999). Molecular cloning and immunolocalization of a novel vertebrate trp homologue from *Xenopus*. *Biochem J* **340**, 593–599.

Borges S, Lindstrom S, Walters C, Warrier A & Wilson M (2008). Discrete influx events refill depleted Ca^{2+} stores in a chick retinal neuron. *J Physiol* **586**, 605–626.

Bouron A, Mbebi C, Loeffler JP & De Waard M (2004). The β-amyloid precursor protein controls a store-operated Ca^{2+} entry in cortical neurons. *Eur J Neurosci* **20**, 2071–2078.

Brandman O, Liou J, Park WS & Meyer T (2007). STIM2 is a feedback regulator that stabilizes basal cytosolic and endoplasmic reticulum Ca^{2+} levels. *Cell* **131**, 1327–1339.

Brereton HM, Harland ML, Auld AM & Barritt GJ (2000). Evidence that the TRP-1 protein is unlikely to account for store-operated Ca^{2+} inflow in *Xenopus laevis* oocytes. *Mol Cell Biochem* **214**, 63–74.

Cadetti L, Bryson EJ, Ciccone CA, Rabl K & Thoreson WB (2006). Calcium-induced calcium release in rod photoreceptor terminals boosts synaptic transmission during maintained depolarization. *Eur J Neurosci* **23**, 2983–2990.

Cadetti L, Tranchina D & Thoreson WB (2005). A comparison of release kinetics and glutamate receptor properties in shaping rod–cone differences in EPSC kinetics in the salamander retina. *J Physiol* **569**, 773–788.

Cheng KT, Liu X, Ong HL & Ambudkar IS (2008). Functional requirement for Orai1 in store-operated TRPC1-STIM1 channels. *J Biol Chem* **283**, 12935–12940.

Chiarini LB, Leal-Ferreira ML, de Freitas FG & Linden R (2003). Changing sensitivity to cell death during development of retinal photoreceptors. *J Neurosci Res* **74**, 875–883.

Choi SY, Borghuis BG, Rea R, Levitan ES, Sterling P & Kramer RH (2005). Encoding light intensity by the cone photoreceptor synapse. *Neuron* **48**, 555–562.

Crousillac S, LeRouge M, Rankin M & Gleason E (2003). Immunolocalization of TRPC channel subunits 1 and 4 in the chicken retina. *Vis Neurosci* **20**, 453–463.

Duncan JL, Yang H, Doan T, Silverstein RS, Murphy GJ, Nune G, Liu X, Copenhagen D, Tempel BL, Rieke F & Krizaj D (2006). Scotopic visual signaling in the mouse retina is modulated by high-affinity plasma membrane calcium extrusion. *J Neurosci* **26**, 7201–7211.

Feske S, Gwack Y, Prakriya M, Srikanth S, Puppel SH, Tanasa B, Hogan PG, Lewis RS, Daly M & Rao A (2006). A mutation in Orai1 causes immune deficiency by abrogating CRAC channel function. *Nature* **441**, 179–185.

Fomina AF & Nowycky MC (1999). A current activated on depletion of intracellular Ca^{2+} stores can regulate exocytosis in adrenal chromaffin cells. *J Neurosci* **19**, 3711–3722.

Garaschuk O, Yaari Y & Konnerth A (1997). Release and sequestration of calcium by ryanodine-sensitive stores in rat hippocampal neurones. *J Physiol* **502**, 13–30.

Gomez TM, Snow DM & Letourneau PC (1995). Characterization of spontaneous calcium transients in nerve growth cones and their effect on growth cone migration. *Neuron* **14**, 1233–1246.

Grynkiewicz G, Poenie M & Tsien RY (1985). A new generation of Ca^{2+} indicators with greatly improved fluorescence properties. *J Biol Chem* **260**, 3440–3450.

Harper JL, Camerini-Otero CS, Li AH, Kim SA, Jacobson KA & Daly JW (2003). Dihydropyridines as inhibitors of capacitative calcium entry in leukemic HL-60 cells. *Biochem Pharmacol* **65**, 329–338.

Heidelberger R, Thoreson WB & Witkovsky P (2005). Synaptic transmission at retinal ribbon synapses. *Prog Retin Eye Res* **24**, 682–720.

Hopf FW, Reddy P, Hong J & Steinhardt RA (1996). A capacitative calcium current in cultured skeletal muscle cells is mediated by the calcium-specific leak channel and inhibited by dihydropyridine compounds. *J Biol Chem* **271**, 22358–22367.

Jia Y, Zhou J, Tai Y & Wang Y (2007). TRPC channels promote cerebellar granule neuron survival. *Nat Neurosci* **10**, 559–567.

Johnson JE Jr, Perkins GA, Giddabasappa A, Chaney S, Xiao W, White AD, Brown JM, Waggoner J, Ellisman MH & Fox DA (2007). Spatiotemporal regulation of ATP and Ca^{2+} dynamics in vertebrate rod and cone ribbon synapses. *Mol Vis* **13**, 887–919.

Jones BW, Watt CB & Marc RE (2005). Retinal remodelling. *Clin Exp Optom* **88**, 282–291.

Kachoei BA, Knox RJ, Uthuza D, Levy S, Kaczmarek LK & Magoski NS (2006). A store-operated Ca^{2+} influx pathway in the bag cell neurons of *Aplysia*. *J Neurophysiol* **96**, 2688–2698.

Kreft M, Krizaj D, Grilc S & Zorec R (2003). Properties of exocytotic response in vertebrate photoreceptors. *J Neurophysiol* **90**, 218–225.

Krizaj D, Bao JX, Schmitz Y, Witkovsky P & Copenhagen DR (1999). Caffeine-sensitive calcium stores regulate synaptic transmission from retinal rod photoreceptors. *J Neurosci* **19**, 7249–7261.

Krizaj D & Copenhagen DR (1998). Compartmentalization of calcium extrusion mechanisms in the outer and inner segments of photoreceptors. *Neuron* **21**, 249–256.

Krizaj D & Copenhagen DR (2002). Calcium regulation in photoreceptors. *Front Biosci* **7**, d2023–d2044.

Krizaj D, Lai FA & Copenhagen DR (2003). Ryanodine stores and calcium regulation in the inner segments of salamander rods and cones. *J Physiol* **547**, 761–774.

Lewis RS (2007). The molecular choreography of a store-operated calcium channel. *Nature* **446**, 284–287.

Liao Y, Erxleben C, Yildirim E, Abramowitz J, Armstrong DL & Birnbaumer L (2007). Orai proteins interact with TRPC channels and confer responsiveness to store depletion. *Proc Natl Acad Sci U S A* **104**, 4682–4687.

Lin JH, Li H, Yasumura D, Cohen HR, Zhang C, Panning B, Shokat KM, Lavail MM & Walter P (2007). IRE1 signaling affects cell fate during the unfolded protein response. *Science* **318**, 944–949.

Lin JH, Walter P & Yen TS (2008). Endoplasmic reticulum stress in disease pathogenesis. *Annu Rev Pathol* **3**, 399–425.

Liu X, Cheng KT, Bandyopadhyay BC, Pani B, Dietrich A, Paria BC, Swaim WD, Beech D, Yildrim E, Singh BB, Birnbaumer L & Ambudkar IS (2007). Attenuation of store-operated Ca^{2+} current impairs salivary gland fluid secretion in TRPC1(–/–) mice. *Proc Natl Acad Sci U S A* **104**, 17542–17547.

Ma R, Rundle D, Jacks J, Koch M, Downs T & Tsiokas L (2003). Inhibitor of mycogenic family, a novel suppressor of store-operated currents through an interaction with TRPC1. *J Biol Chem* **278**, 52763–52772.

Mercurio AM & Holtzman E (1982). Smooth endoplasmic reticulum and other agranular reticulum in frog retinal photoreceptors. *J Neurocytol* **11**, 263–293.

Morgans CW, El Far O, Berntson A, Wässle H & Taylor WR (1998). Calcium extrusion from mammalian photoreceptor terminals. *J Neurosci* **18**, 2467–2474.

Neher E (1995). The use of fura-2 for estimating Ca buffers and Ca fluxes. *Neuropharmacology* **34**, 1423–1442.

Nohmi M, Hua SY & Kuba K (1992). Basal Ca^{2+} and the oscillation of Ca^{2+} in caffeine-treated bullfrog sympathetic neurones. *J Physiol* **450**, 513–528.

Ong HL, Cheng KT, Liu X, Bandyopadhyay BC, Paria BC, Soboloff J, Pani B, Gwack Y, Srikanth S, Singh BB, Gill DL & Ambudkar IS (2007). Dynamic assembly of TRPC1-STIM1-Orai1 ternary complex is involved in store-operated calcium influx. Evidence for similarities in store-operated and calcium release-activated calcium channel components. *J Biol Chem* **282**, 9105–9116.

Parekh AB & Putney JW Jr (2005). Store-operated calcium channels. *Physiol Rev* **85**, 757–810.

Prakash YS, Iyanoye A, Ay B, Mantilla CB & Pabelick CM (2006). Neurotrophin effects on intracellular Ca^{2+} and force in airway smooth muscle. *Am J Physiol Lung Cell Mol Physiol* **291**, L447–L456.

Putney JW Jr (1990). Capacitative calcium entry revisited. *Cell Calcium* **11**, 611–624.

Rea R, Li J, Dharia A, Levitan ES, Sterling P & Kramer RH (2004). Streamlined synaptic vesicle cycle in cone photoreceptor terminals. *Neuron* **41**, 755–766.

Rieke F & Schwartz EA (1994). A cGMP-gated current can control exocytosis at cone synapses. *Neuron* **13**, 863–873.

Rieke F & Schwartz EA (1996). Asynchronous transmitter release: control of exocytosis and endocytosis at the salamander rod synapse. *J Physiol* **493**, 1–8.

Roos J, DiGregorio PJ, Yeromin AV, Ohlsen K, Lioudyno M, Zhang S, Safrina O, Kozak JA, Wagner SL, Cahalan MD, Veliçelebi G & Stauderman KA (2005). STIM1, an essential and conserved component of store-operated Ca^{2+} channel function. *J Cell Biol* **169**, 435–445.

Sakaki Y, Sugioka M, Fukuda Y & Yamashita M (1997). Capacitative Ca^{2+} influx in the neural retina of chick embryo. *J Neurobiol* **32**, 62–68.

Schmitz Y & Witkovsky P (1996). Glutamate release by the intact light-responsive photoreceptor layer of the *Xenopus* retina. *J Neurosci Methods* **68**, 55–60.

Schmitz Y & Witkovsky P (1997). Dependence of photoreceptor glutamate release on a dihydropyridine-sensitive calcium channel. *Neuroscience* **78**, 1209–1216.

Shim S, Goh EL, Ge S, Sailor K, Yuan JP, Roderick HL, Bootman MD, Worley PF, Song H & Ming GL (2005). XTRPC1-dependent chemotropic guidance of neuronal growth cones. *Nat Neurosci* **8**, 730–735.

Shoshan-Barmatz V, Zakar M, Shmuelivich F, Nahon E & Vardi N (2007). Retina expresses a novel variant of the ryanodine receptor. *Eur J Neurosci* **26**, 3113–3125.

Smyth JT, Dehaven WI, Jones BF, Mercer JC, Trebak M, Vazquez G & Putney J Jr (2006). Emerging perspectives in store-operated Ca^{2+} entry: roles of Orai, Stim and TRP. *Biochim Biophys Acta* **1763**, 1147–1160.

Soboloff J, Spassova MA, Dziadek MA & Gill DL (2006). Calcium signals mediated by STIM and Orai proteins – a new paradigm in inter-organelle communication. *Biochim Biophys Acta* **1763**, 1161–1168.

Suryanarayanan A & Slaughter MM (2006). Synaptic transmission mediated by internal calcium stores in rod photoreceptors. *J Neurosci* **26**, 1759–1766.

Szikra T & Krizaj D (2006). The dynamic range and domain-specific signals of intracellular calcium in photoreceptors. *Neuroscience* **141**, 143–155.

Szikra T & Krizaj D (2007). Intracellular organelles and calcium homeostasis in rods and cones. *Vis Neurosci* **24**, 733–743.

Thoreson WB, Nitzan R & Miller RF (1997). Reducing extracellular Cl^- suppresses dihydropyridine-sensitive Ca^{2+} currents and synaptic transmission in amphibian photoreceptors. *J Neurophysiol* **77**, 2175–2190.

Thoreson WB, Rabl K, Townes-Anderson E & Heidelberger R (2004). A highly Ca^{2+}-sensitive pool of vesicles contributes to linearity at the rod photoreceptor ribbon synapse. *Neuron* **42**, 595–605.

Thoreson WB, Tranchina D & Witkovsky P (2003). Kinetics of synaptic transfer from rods and cones to horizontal cells in the salamander retina. *Neuroscience* **122**, 785–798.

Usachev YM & Thayer SA (1999). Ca^{2+} influx in resting rat sensory neurones that regulates and is regulated by ryanodine-sensitive Ca^{2+} stores. *J Physiol* **519**, 115–130.

Vig M, DeHaven WI, Bird GS, Billingsley JM, Wang H, Rao PE, Hutchings AB, Jouvin MH, Putney JW & Kinet JP (2008). Defective mast cell effector functions in mice lacking the CRACM1 pore subunit of store-operated calcium release-activated calcium channels. *Nat Immunol* **9**, 89–96.

Wang GX & Poo MM (2005). Requirement of TRPC channels in netrin-1-induced chemotropic turning of nerve growth cones. *Nature* **434**, 898–904.

Worley PF, Zeng W, Huang GN, Yuan JP, Kim JY, Lee MG & Muallem S (2007). TRPC channels as STIM1-regulated store-operated channels. *Cell Calcium* **42**, 205–211.

Wu X, Zagranichnaya TK, Gurda GT, Eves EM & Villereal ML (2004). A TRPC1/TRPC3-mediated increase in store-operated calcium entry is required for differentiation of H19–7 hippocampal neuronal cells. *J Biol Chem* **279**, 43392–43402.

Yang J, Pawlyk B, Wen XH, Adamian M, Soloviev M, Michaud N, Zhao Y, Sandberg MA, Makino CL & Li T (2007). Mpp4 is required for proper localization of plasma membrane calcium ATPases and maintenance of calcium homeostasis at the rod photoreceptor synaptic terminals. *Hum Mol Genet* **16**, 1017–1029.

Yuan JP, Zeng W, Huang GN, Worley PF & Muallem S (2007). STIM1 heteromultimerizes TRPC channels to determine their function as store-operated channels. *Nat Cell Biol* **9**, 636–645.

Zagranichnaya TK, Wu X & Villereal M (2005). *J Biol Chem* **280**, 29559–29569.

Zhang SL, Kozak JA, Jiang W, Yeromin AV, Chen J, Yu Y, Penna A, Shen W, Chi V & Cahalan MD (2008). Store-dependent and -independent modes regulating Ca^{2+} release-activated Ca^{2+} channel activity of human Orai1 and Orai3. *J Biol Chem* **283**, 17662–17671.

Zhu X, Jiang M, Peyton M, Boulay G, Hurst R, Stefani E & Birnbaumer L (1996). trp, a novel mammalian gene family essential for agonist-activated capacitative Ca^{2+} entry. *Cell* **85**, 661–671.

Zitt C, Zobel A, Obukhov AG, Harteneck C, Kalkbrenner F, Lückhoff A & Schultz G (1996). *Neuron* **16**, 29559–29563.

Acknowledgements

The work was supported by a grant from the Hungarian Eötvös Fellowship, the Knights Templar Foundation (T.S., P.B and K.C.), That Man May See Foundation (D.K.), National Institutes of Health grants to D.K. (EY13870) and W.B.T. (EY10542), Sabbatical Research Grant from Research to Prevent Blindness (W.B.T.) and Foundation Fighting Blindness (D.K.). The research was also supported by unrestricted grants from Research to Prevent Blindness to the Moran Eye Institute, UCSF Department of Ophthalmology and UNMC Department of Ophthalmology and Visual Sciences. We would like to thank Ms Elizabeth Hawkins for the help with Western blots, Dr Helen Huang for help with RNAi experiments and Dr Leonidas Tsiokas (University of Oklahoma Health Sciences Center) for the generous gift of the xTRP antibody. We thank David Copenhagen and his lab at UCSF for fruitful discussions.

Authors' present addresses

Tamas Szikra: Friedrich Miescher Institute, Basel 4048, Switzerland.

K. Cusato: Biomedical & Chemical Engineering Department, SUNY, Syracuse, NY 13244, USA.

Supplemental material

Online supplemental material for this paper can be accessed at: http://jp.physoc.org/cgi/content/full/jphysiol.2008.160051/DC1